

Behavior and Strength of Slab-Edge Beam-Column Connections under Shear Force and Moment

Omar M. Ben-Sasi

Abstract—A total of fourteen slab-edge beam-column connection specimens were tested gradually to failure under the effect of simultaneous action of shear force and moment. The objective was to investigate the influence of some parameters thought to be important on the behavior and strength of slab-column connections with edge beams encountered in flat slab flooring and roofing systems. The parameters included the existence and strength of edge beam, depth and width of edge beam, steel reinforcement ratio of slab, ratio of moment to shear force, and the existence of openings in the region next to the column.

Results obtained demonstrated the importance of the studied parameters on the strength and behavior of slab-column connections with edge beams.

Keywords—Strength, flat slab, slab-column connections, shear force, moment, behavior.

I. INTRODUCTION

REINFORCED concrete flat slab roofs and floors are becoming increasingly popular in the building industry for several advantages over the traditional slab-beam system. However, a major problem associated with a flat slab system is its susceptibility to a local failure at a slab-column connection known as punching shear failure. The chance of punching failure increases as the shearing effects increase around a connection as for the case of slab-exterior column connections due to, at least, the geometric unsymmetry. Previous experimental studies [1]-[3] indicated increasing weakness of exterior connections as the ratio of the moment normal to slab edge, known as unbalanced moment, to shear force increases. On the other hand, the column aspect ratio and the flexural reinforcement ratio normal to the slab edge were found in favor of increasing connection shear strength [3]. Studies [3]-[5], conducted on specimens of slab-edge column connections with spandrel beams, proved the use of such beams to be very effective in increasing the punching shear strength of edge connections.

In this study, more insight is introduced concerning the influence of the spandrel beam on edge connections by studying different slab and spandrel beam parameters.

A. Research Significance

The present experimental study has provided useful data regarding the strength and behavior of slab-edge column connections with spandrel beams which as of yet are still

meager. These data should help, when utilized, in the development and assessment of methods for predicting the punching shear strength of slab-edge column connections with spandrel beams.

B. Experimental Program

An experimental program was designed to study the behavior and ultimate strength of slab-column connections with spandrel beams by testing, to failure, some specimens approximately simulating connections around edge columns with spandrel beams. The parameters included in the study were: 1. spandrel beam presence; 2. beam depth; 3. beam width; 4. beam torsional strength, through variation in stirrup spacing; 5. slab flexural reinforcement around the column; 6. Moment to shear ratio, M/V ; and 7. the presence of two openings next to column corners.

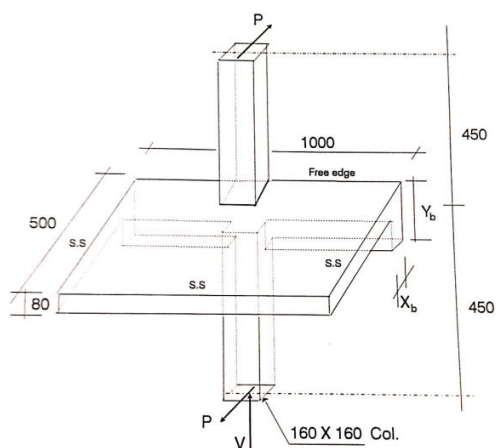
C. Test Specimens

A total of fourteen, half-scale specimens were tested. These specimens were, designated as SE-1, SE-2,...through SE-14. Specimens SE-1 through SE-9, SE-12 and SE-14 consisted of two column stubs monolithically cast with the slab-spandrel part, Fig. 1. The slab-spandrel part is assumed approximately bounded by the lines of contraflexure in a prototype flat plate structure with spandrel beam. Specimens SE-10 and SE-13 did not contain spandrel beams while specimen SE-11 had a spandrel beam but no slab. Detailed information regarding dimensions and reinforcement ratios is given in Table I of test specimens. More detailed data of the test specimens is found elsewhere [6].

D. Materials

The concrete used for all specimens consisted of ordinary Portland cement, sand, and gravel of 12mm maximum nominal size. The longitudinal reinforcement of spandrel beams and the slab mats consisted of 8mm in diameter plain steel bars of yield strength equal to 2980kg/cm². The longitudinal reinforcement used for column stubs consisted of 12mm plain bars. Stirrup reinforcement of the spandrel beams and column stubs was made of 6 mm plain bars of yield strength equal to 3100kg/cm². These strength values were the average of three sample values for each bar size. The column stubs were made and intended to be strong enough to avoid any possible column failure during testing.

Omar M. Ben-Sasi is Prof. of Civil Engineering at the Civil Engineering Department, University of Misurata, Misurata, Libya (e-mail: obensasi@yahoo.com).



All Dimensions are in mm.

Fig. 1 Slab-beam –column connection specimen

E. Instrumentation

Strains of some selected tension bars within the column vicinity of the slab and spandrel beam were obtained using strain gages connected to a digital strain indicator system. The gages were fixed by special cement onto carefully cleaned positions on the selected steel bars in the vicinity of the column. The strain indicator system had strain accuracy in the order of one microstrain.

Concrete strains in the column vicinity were obtained by means of a demec strain gage having a 50mm gage length. The gage was accurate in the order of 0.000025. It measures strains through using stainless steel discs with prepared holes suitable for mounting the gage on position where measurements to be taken. The discs were fixed onto the specimen compression side using special adhesive cement and spaced at the gage length of 50mm. To ensure good contact of the discs to concrete, the specimens were left for at least an overnight before testing.

Dial deflection gages of 0.01mm accuracy were used for the deflection measurements on certain positions to enable measurements of slab deflection, column stub displacement, and connection rotation.

F. Loading System and Equipment

The tested specimens of this experimental work were loaded through their column stubs as shown in Fig. 1. The loading arrangement as such was intended to produce a case of transfer of shear force and unbalanced moment at the connection. The axial load and the couple loads were furnished respectively by means of a 25-ton capacity and 10-ton capacity hydraulic jacks. Loads were measured by means of proper load cells placed between the hydraulic jacks and the points of load application.

TABLE I
STUDY VARIABLES OF TESTED SPECIMENS

| Study Variable | specimen | f'_c MPa | M/V m. | Beam width (mm) | | Closed stirrup Dimensions (mm) | | | T_n Kn.m | $\rho\%$ |
|-------------------|-------------|---------------|-----------|-----------------|-------|--------------------------------|-------|-----|---------------|----------|
| | | | | X_b | Y_b | X_1 | Y_1 | S | | |
| Presence Of | SE-9 | 18.6 | 0.36 | 100 | 240 | 65 | 200 | 80 | 5.6 | 1.11 |
| | SE-10 | 19.6 | 0.36 | --- | -- | --- | --- | --- | --- | 1.11 |
| Spandrel T_n | SE-11 | 18.2 | 0.36 | 100 | 240 | 65 | 200 | 80 | 5.6 | --- |
| | SE-1 | 17.7 | 0.36 | 100 | 160 | 65 | 125 | 50 | 5.6 | 1.47 |
| Beam Depth | SE-2 | 23.8 | 0.36 | 100 | 160 | 65 | 125 | 100 | 2.8 | 1.47 |
| | SE-1 | 17.7 | 0.36 | 100 | 160 | 65 | 125 | 50 | 5.6 | 1.47 |
| Beam Width | SE-3 | 20.4 | 0.36 | 100 | 240 | 65 | 200 | 80 | 5.6 | 1.47 |
| | SE-4 | 21.6 | 0.36 | 100 | 300 | 65 | 250 | 100 | 5.6 | 1.47 |
| ρ | SE-12 | 19.4 | 0.34 | 100 | 240 | 65 | 200 | 60 | 7.5 | 1.47 |
| | SE-5 | 20.3 | 0.36 | 125 | 240 | 85 | 200 | 80 | 7.3 | 1.47 |
| M/V | SE-6 | 20.5 | 0.36 | 150 | 240 | 110 | 200 | 100 | 7.6 | 1.47 |
| | SE-9 | 18.6 | 0.36 | 100 | 240 | 65 | 200 | 80 | 5.6 | 1.11 |
| Opening | SE-3 | 20.4 | 0.36 | 100 | 240 | 65 | 200 | 80 | 5.6 | 1.47 |
| | SE-7 | 19.9 | 0.36 | 100 | 240 | 65 | 200 | 80 | 5.6 | 1.66 |
| Opening | SE-8 | 17.9 | 0.36 | 100 | 240 | 65 | 200 | 80 | 5.6 | 1.84 |
| | SE-3 | 20.4 | 0.36 | 100 | 240 | 65 | 200 | 80 | 5.6 | 1.47 |
| Opening | SE-14 | 20.9 | 0.54 | 100 | 240 | 65 | 200 | 80 | 5.6 | 1.47 |
| | SE-10 (no) | 19.6 | 0.36 | --- | -- | --- | --- | --- | --- | 1.11 |
| | SE-13 (yes) | 20.8 | 0.36 | --- | -- | --- | --- | --- | --- | 1.11 |

G. Testing Procedure

Each specimen to be tested was put in position in the testing frame and leveled accurately such that the slab was oriented vertically and the column stubs horizontally as depicted in Fig. 3. Having the steel discs fixed onto the compression side of the slab long enough before testing, the dial gages set in

proper locations, and the electrical strain gages and load cells connected to the strain indicator, zero readings were taken. Monotonic loading, then, was applied to each specimen in increments. For specimens SE-1 through SE-9 and SE-12 the increments were in 0.5 ton for the axial load followed by a 0.2-ton increment for each of the two lateral loads that

produced the unbalanced moment action on the specimen. For specimens SE-10, SE-11, and SE-13, which were obviously of low strength compared to the others, half of these increments were used. The load increments as such produced a moment to axial force ratio of 0.36m, where the couple arm was 0.9m for the tested specimens, see Fig. 1. For SE-14 the lateral load increment was 0.3t which produced a moment to axial load ratio of 0.54m for that specimen. The mentioned increments were kept up to about 80% of the expected ultimate loads. Afterwards they were halved. This reduction was to lessen the effect of nonlinearity in the relationship between load and displacement that prevails at this level of loading. Throughout loading stages, as load was increased, a record was made of the different strain and deflection measurements. The performance of the testing frame and equipment were watched carefully during loading.

II. GENERAL BEHAVIOR OF TESTED SPECIMENS

The specimens SE-1 through SE-9, SE-12, and SE-14 were slab-beam-column connections. These specimens exhibited basically the same shape of cracking pattern upon loading and same final mode of failure. But they differed, however, in the intensity and width of cracks at different loading stages as a result of differences in the affecting parameters. The first crack in all of these specimens was a flexural-type crack. It occurred at the tension side of the slab at its interface with the inner column face and it turned to have the maximum width relative to other cracks that occurred later on. Further increase in loading caused this crack to turn around the two inner corners of the column and cross the spandrel beam upper face in an inclined direction due to torsion effects prevailing therein. As loading was increased the crack became wider and extended, at both column sides, to the outer face of spandrel beam in an inclined direction as was the case on the upper face. Besides, more flexural cracks, in the form of lines radiating from the column, and inclined torsion cracks, on the beam faces, formed. It is worth mentioning here that cracks on the inner beam face were noticed to be small in width and few in number relative to those on the upper and outer faces. The inclination angle of the torsion cracks was noticed to be about 45° with respect to the spandrel beam axis. A typical crack pattern is shown in Fig. 2, for specimen SE-12.



Fig. 2 Crack pattern as exhibited by Se-12

Loading of specimens close to their ultimate capacity caused the firstly appeared cracks at the inner slab-column interface and on the beam upper and outer faces to widen noticeably. This resulted in a remarkable increase in the rotation of the column stub along with the adjoined parts of slab and beam that were bounded by these said major cracks at both sides of the column stub, relative to the rest of the test specimen. The ultimate capacity was soon reached afterwards when large rotations were noticed with virtually no load increase. Concrete crushing, then, took place at the compression region of the inner slab-column interface and at the compression side of the spandrel beam accompanied with load decrease and remarkable rotation increase of the column stubs. As a result, the stubs punched through the slab at the common inner interface. The ultimate axial loads and unbalanced moments transferred through the different specimen connections are presented in Table II. By noting strains of steel bars at different loading stages it was found out that the bars crossing the column inner face and then the tension longitudinal bars of the spandrel steel yielded before the ultimate capacity of the tested specimens was reached. The above described behavior reveals, then, that these specimens failed primarily in a flexural-torsion mode followed by punching of the column stubs through the slab.

Specimen SE-10 was a slab-column connection with no spandrel beam. It had the same slab as that of the specimen SE-9. The first crack appeared was also a flexural crack at the tension region of the inner slab-column interface. The crack turned around the inner column corners to cross the top side of the torsion strip (part of the slab that crosses the column stub in the lateral direction and of a width equal to the column depth). The crack was inclined at an angle of about 60° relative to moment vector at the top side of the strip and 45° at its free edge. At a loading level of about 70% of the ultimate an important crack was noticed in front of the inner column face on the tension side of the slab and parallel to the first flexural crack. This crack was located at about the slab depth from the column face. This crack was believed to be due to the diagonal tension crack produced within the slab depth and this location represents the bottom tip of it close to the surface of the slab. Further increase of loading caused more cracks to appear on the specimen and the old ones to widen noticeably due to yielding of tension steel bars crossing the column inner and side faces. Ultimately, the specimen was found to fail primarily in a flexural-torsion mode followed by punching of the column stub through the slab. Specimen SE-13 differed from SE-10 in that it had two 120x80mm. openings located next to the inner corners.

TABLE II
TEST RESULTS OF TESTED SPECIMENS

| Study Variable | specimen | f_c' MPa | M/V | Beam width | Beam depth | Closed stirrup dimensions (mm) | | | T_n Kn.m | $\rho\%$ | V Kn. | M Kn.m |
|----------------|-----------------|---------------|------|---------------|---------------|--------------------------------|-------|-----|---------------|----------|----------|-----------|
| | | | | (mm) X_b | (mm) Y_b | X_1 | Y_1 | S | | | | |
| Presence | SE-9 | 18.6 | 0.36 | 100 | 240 | 65 | 200 | 80 | 5.6 | 1.11 | 49.1 | 17.7 |
| Of | SE-10 | 19.6 | 0.36 | --- | -- | --- | --- | --- | --- | 1.11 | 31.9 | 11.5 |
| Spandrel | SE-11 | 18.2 | 0.36 | 100 | 240 | 65 | 200 | 80 | 5.6 | --- | 13.7 | 4.9 |
| T_n | SE-1 | 17.7 | 0.36 | 100 | 160 | 65 | 125 | 50 | 5.6 | 1.47 | 49.1 | 17.7 |
| | SE-2 | 23.8 | 0.36 | 100 | 160 | 65 | 125 | 100 | 2.8 | 1.47 | 44.1 | 15.9 |
| Beam | SE-1 | 17.7 | 0.36 | 100 | 160 | 65 | 125 | 50 | 5.6 | 1.47 | 49.1 | 17.7 |
| Depth | SE-3 | 20.4 | 0.36 | 100 | 240 | 65 | 200 | 80 | 5.6 | 1.47 | 54.0 | 19.4 |
| | SE-4 | 21.6 | 0.36 | 100 | 300 | 65 | 250 | 100 | 5.6 | 1.47 | 58.9 | 21.2 |
| Beam | SE-12 | 19.4 | 0.34 | 100 | 240 | 65 | 200 | 60 | 7.5 | 1.47 | 56.4 | 19.4 |
| Width | SE-5 | 20.3 | 0.36 | 125 | 240 | 85 | 200 | 80 | 7.3 | 1.47 | 63.8 | 23.0 |
| | SE-6 | 20.5 | 0.36 | 150 | 240 | 110 | 200 | 100 | 7.6 | 1.47 | 71.1 | 25.6 |
| | SE-9 | 18.6 | 0.36 | 100 | 240 | 65 | 200 | 80 | 5.6 | 1.11 | 49.1 | 17.7 |
| ρ | SE-3 | 20.4 | 0.36 | 100 | 240 | 65 | 200 | 80 | 5.6 | 1.47 | 54.0 | 19.4 |
| | SE-7 | 19.9 | 0.36 | 100 | 240 | 65 | 200 | 80 | 5.6 | 1.66 | 54.0 | 19.4 |
| | SE-8 | 17.9 | 0.36 | 100 | 240 | 65 | 200 | 80 | 5.6 | 1.84 | 56.4 | 20.3 |
| M/V | SE-3 | 20.4 | 0.36 | 100 | 240 | 65 | 200 | 80 | 5.6 | 1.47 | 54.0 | 19.4 |
| | SE-14 | 20.9 | 0.54 | 100 | 240 | 65 | 200 | 80 | 5.6 | 1.47 | 27.0 | 14.6 |
| Openings | SE-10 (no) | 19.6 | 0.36 | --- | -- | --- | --- | --- | --- | 1.11 | 31.9 | 11.5 |
| | SE-13 (present) | 20.8 | 0.36 | --- | -- | --- | --- | --- | --- | 1.11 | 22.1 | 7.95 |

The cracking, again, started as flexural at the inner column-slab interface and then was followed by the inclined torsion cracking at the torsion strips at both column sides. The specimen also failed primarily at the ultimate conditions in a flexural-torsion mode followed immediately by punching of the column through the slab. Ultimate loads carried by connections SE-10 and SE-13 are given in Table II.

Specimen SE-11 was a column-spandrel beam connection with no slab. The spandrel beam was identical to that of SE-9. Upon loading the beam cracked first at its tension side in an inclined direction relative to beam axis then cracked at the outer face. Further increase of loading resulted in widening of these cracks and the development of new cracks at both sides of the column stub. This in turn caused remarkable rotations of the column stub and the adjoined beam parts that were bounded by the major inclined cracks at the two column sides. Ultimately, the beam failed in a torsion mode. Ultimate loads carried are given in Table II.

III. INFLUENCE OF STUDIED PARAMETERS

In this section it is aimed at presenting the influence of the studied parameters on connection ultimate capacities, stiffness, and ductility. Test recorded ultimate capacities are presented in Table II. Displacement and rotational stiffness for different test specimen connections were compared. This was done by comparing the steepness of graphs such as those shown in Figs. 3 (a) and (b) for axial load against column displacement and moment against connection rotation respectively. The conclusions drawn from that comparison are reported herein.

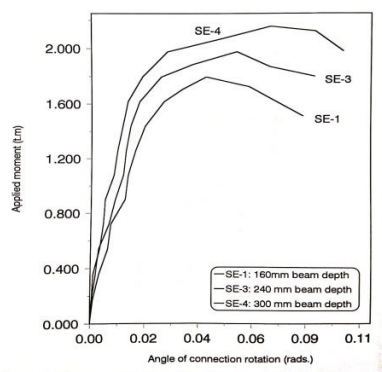


Fig. 3 (a) Axial load versus axial disp

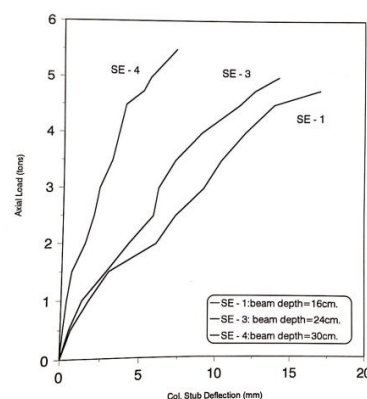


Fig. 3 (b) Moment versus connection rotation

A. Presence of a Spandrel Beam

SE-9 was a slab-beam-column connection with a spandrel beam depth of 240 mm (three times slab depth). SE-10 was only a slab-column connection while SE-11 was a beam-column connection. The slab of SE-9 was identical to that of SE-10 and its beam was identical to that of SE-11. This helped in making the needed comparisons. Connection displacement and rotational stiffness of SE-9, with spandrel beam, were higher than those of SE-10, without spandrel. From Table II it can be seen that the presence of a spandrel in SE-9 resulted in about 54% increase in ultimate capacity relative to SE-10. Moreover, from the same table it can be noticed that the ultimate capacity of SE-9 has been higher than the sum of the individual capacities of SE-10 and SE-11. This may be interpreted on the basis that the spandrel displacement is more restricted when the spandrel acts as connected to the adjacent slab in SE-9 rather than as isolated in SE-11.

B. Spandrel Beam Torsion Strength

The nominal pure torsion strength, T_n of a spandrel beam is given by the equation $T_n = 2A_w f_{wy} X_1 Y_1 / S$ [7]. Where, A_w = cross sectional area of one branch of a stirrup, f_{wy} = yield strength of stirrup steel, X_1 = length of the horizontal branch of a stirrup, Y_1 = length of the vertical branch of a stirrup, and S = spacing between stirrups. The specimens tested in this work had two spandrel beam sections that are connected with the column stub from both sides. So double the value of T_n is considered in the calculation of torsion strength for the tested specimens. SE-1 and SE-2 were made to differ only in spacing of stirrups which in SE-2 was double that in SE-1. Hence, making T_n of SE-1 double that of SE-2. The two specimens exhibited, virtually, the same displacement and rotational stiffness before cracking. Beyond that load level, displacement and rotational stiffness of SE-1 became markedly greater than those of SE-2 which proves effectiveness of increasing T_n on connection stiffness. Referring to Table II, it can be seen that as the torsion strength was increased, the ultimate capacity increased.

C. Spandrel Beam Depth

This variable was studied through specimens SE-1, SE-3 and SE-4 whose beam depths were 160mm, 240mm and 300 mm respectively. As the beam depth was increased, the displacement stiffness increased considerably. The rotational stiffness increased also but by a lesser amount. From Table II, it can be noticed that the ultimate capacity increased as the beam depth was increased.

D. Spandrel Beam Width

This variable was studied through specimens SE-12, SE-5, and SE-6 whose beam depths were 100mm, 125mm and 150 mm respectively. As the beam width was increased the displacement and rotational stiffness increased. The ultimate capacity increased also as can be seen from Table II.

E. Steel Ratio, ρ , of Top Bars Crossing Spandrel Beam

The steel ratio, ρ , is the ratio of the top tension steel crossing the spandrel beam (the steel bars crossing the inner column side were kept the same, $4 \phi 8$ mm, for all specimens tested in this work).

The specimens for the study of the effect of this variable were SE-3, SE-7, SE-8 and SE-9 for which ρ was 0.0147, 0.0166, 0.0184 and 0.011 respectively. Both of displacement and rotational stiffness increased as the ratio ρ was increased. As can be seen from Table II, increasing ρ is more effective in increasing the connection capacity at low values of the ratio ρ than at high values. This should indicate that certain limit for ρ exists beyond which no more increase in capacity would be expected as ρ increases.

F. Effect of the M/V Ratio

The specimens of this parameter were SE-3 and SE-14. The former specimen had an M/V ratio equal to 0.36m and the latter specimen had 0.54m ratio, 50% higher. By comparing graphs similar to those of Fig. 3, increasing this variable was found to considerably decrease the rotational stiffness and to a lesser extent the displacement stiffness. From Table II, it can be seen that ultimate capacity had markedly decreased as M/V increased.

G. Effect of the Presence of Openings Next to Column Inner Corners

SE-10 and SE-13 were the specimens tested for this variable. The two specimens were identical slab-edge column connections except for the presence of two, 120x80mm, and openings next to the two inner corners of SE-13. The loss of confinement at column corners due to presence of openings in SE-13 resulted in a high decrease in displacement and rotational stiffness compared to SE-10. From Table II, it can be seen that an appreciable drop in ultimate capacity of about 31% of that of SE-10 has occurred as a result of the presence of the openings in SE-13.

IV. CONCLUSIONS

The important conclusions that can be drawn from the reported results of the tests run for this investigation are:

1. The spandrel beam is very effective in enhancing the strength of a slab-column connection. The connection strength increases as the beam torsion strength, and beam cross section dimensions are increased.
2. The strength of a slab-column connection increases to a certain limit by increasing the tension steel crossing the spandrel beam.
3. The connection strength significantly decreases as the M / V ratio is increased.

REFERENCES

- [1] Zaghoul, E. R. F., "Strength and Behavior of Corner and Edge Column-Slab Connections in Reinforced Concrete Flat Plates," Thesis presented to The University of Calgary, Calgary, Alberta, Canada in partial

fulfillment of the requirements for the degree of Doctor of Philosophy in Civil Engineering in 1971.

- [2] Zidan, S., "Strength and Behavior of slab-column connections," M.Sc. Thesis, University of Alexandria, Egypt, 1981.
- [3] Rangan, B. V, "Tests on Slabs in the Vicinity of Edge Columns," A. C. I. Structural Journal V. 87, No. 6, November-March 1990, pp. 623 - 629.
- [4] El-Sheikh, A. I., "Effect of Spandrel Beam on Strength and Behavior of Column-Floor Connections," M.Sc. Thesis, University of Alexandria, Egypt, 1988.
- [5] Falamaki, M. and Loo, Y. C., "Punching Shear Tests of Half - Scale Reinforced Concrete Models with Spandrel Beams," ACI Structural Journal, May - June 1992 , pp. 263 - 271.
- [6] Ben-Sasi, Omar M., "Interaction between Exterior and Interior Columns and Concrete Slabs," Ph.D. Thesis presented to The University of Alexandria, Alex., Egypt for the Degree of Doctor of Philosophy in Civil Engineering in 1999.
- [7] Hsu, T. T. C. "Torsion of Reinforced Concrete," VNR, New York 1984.